

Feedback regulation by Atf3 in the endothelin-1-responsive transcriptome of cardiomyocytes: Egr1 is a principal Atf3 target

Article

Accepted Version

Giraldo, A., Barrett, O. P. T., Tindall, M. J., Fuller, S. J., Amirak, E., Bhattacharya, B. S., Sugden, P. H. and Clerk, A. ORCID: <https://orcid.org/0000-0002-5658-0708> (2012) Feedback regulation by Atf3 in the endothelin-1-responsive transcriptome of cardiomyocytes: Egr1 is a principal Atf3 target. *Biochemical Journal*, 444 (2). pp. 343-355. ISSN 0264-6021 doi: 10.1042/BJ20120125 Available at <https://centaur.reading.ac.uk/27916/>

It is advisable to refer to the publisher's version if you intend to cite from the work. See [Guidance on citing](#).

To link to this article DOI: <http://dx.doi.org/10.1042/BJ20120125>

Publisher: Portland Press Limited

Publisher statement: The final version of record is available at <http://www.biochemj.org/bj/444/bj4440343.htm>

All outputs in CentAUR are protected by Intellectual Property Rights law, including copyright law. Copyright and IPR is retained by the creators or other

copyright holders. Terms and conditions for use of this material are defined in the [End User Agreement](#).

www.reading.ac.uk/centaur

CentAUR

Central Archive at the University of Reading

Reading's research outputs online

Feedback regulation by Atf3 in the endothelin-1-responsive transcriptome of cardiomyocytes: Egr1 is a principal Atf3 target

Alejandro Giraldo*§, Oliver P.T. Barrett†§, Marcus J. Tindall*‡, Stephen J. Fuller*, Emre A. Amirak*, Bonhi S. Bhattacharya‡, Peter H. Sugden*, Angela Clerk¹*

* Institute of Cardiovascular and Metabolic Research, School of Biological Sciences, University of Reading, Whiteknights, Reading RG6 6BX, UK.

† Department of Life Sciences, Imperial College London, London SW7 2AZ, UK.

‡ Department of Mathematics & Statistics, University of Reading, Whiteknights, PO Box 220, Reading, RG6 6AX, UK.

§ These authors contributed equally to this study.

¹ To whom correspondence should be addressed (email a.clerk@reading.ac.uk).

Synopsis

Endothelin-1 promotes cardiomyocyte hypertrophy by inducing changes in gene expression. Immediate early genes including activating transcription factor 3 (Atf3), Egr1 and Ptgs2 are rapidly and transiently upregulated by endothelin-1 in cardiomyocytes. Atf3 regulates expression of downstream genes and is implicated in negative feedback regulation of other immediate early genes. To identify Atf3-regulated genes, we knocked down Atf3 expression in cardiomyocytes exposed to endothelin-1 and used microarrays to interrogate the transcriptomic effects. Of upregulated mRNAs, expression of 23 (including Egr1, Ptgs2) was enhanced and expression of 25 was inhibited by Atf3 knockdown. Using quantitative PCR, we determined that knockdown of Atf3 had little effect on upregulation of Egr1 mRNA over 30 min, but abolished the subsequent decline, causing sustained Egr1 mRNA expression and enhanced protein expression. This resulted from direct binding of Atf3 to the Egr1 promoter. Mathematical modelling established that Atf3 can suffice to suppress Egr1 expression. Given the widespread co-regulation of Atf3 with Egr1, we suggest that the Atf3-Egr1 negative feedback loop is of general significance. Loss of Atf3 caused abnormal cardiomyocyte growth, presumably resulting from dysregulation of target genes. Our data therefore identify Atf3 as a nexus in cardiomyocyte hypertrophy required to facilitate the full and proper growth response.

Short title: Feedback regulation by Atf3

Keywords: Activating transcription factor 3, immediate early genes, negative feedback, cyclooxygenase 2, microarrays, hypertrophy.

Abbreviations used: Adenovirus, AdV; antisense, AS; chromatin immunoprecipitation, ChIP; endothelin-1, ET-1; extracellular signal-regulated kinase, ERK; Gq protein-coupled receptor, GqPCR; immediate early gene, IEG; interleukin, IL; mitogen-activated protein kinase, MAPK; multiplicity of infection, MOI.

INTRODUCTION

Cardiomyocytes, the terminally-differentiated contractile cells of the heart, undergo hypertrophy (i.e. increase in cell size) in response to Gq protein-coupled receptor (GqPCR) agonists including endothelin-1 (ET-1) [1]. ET-1 particularly activates the extracellular signal-regulated kinase 1/2 (ERK1/2) cascade, a pathway that is associated with cardiomyocyte hypertrophy [1,2]. ERK1/2 signalling is strongly implicated in transcriptional regulation and elicits many longer term effects through changes in gene expression [3]. Perhaps unsurprisingly therefore, ~70% of the changes in gene expression induced in neonatal rat cardiomyocytes over the first 4 h of stimulation with ET-1 requires ERK1/2 signalling [4-6]. However, activation of ERK1/2 in cardiomyocytes by ET-1 is rapid and transient [7], and this phase may be viewed as an initiating trigger of the longer term response. Consistent with this, exposure of cardiomyocytes to ET-1 results in multiphasic patterns of gene expression that presumably culminate in hypertrophic growth [5]. Our previous studies identified a number of immediate early genes (IEGs; genes that are regulated by pre-existing transcription factors) that are particularly rapidly upregulated in cardiomyocytes exposed to ET-1 including activating transcription factor 3 (Atf3) [5].

Atf3 is a member of the ATF/CREB family proteins which bind as homo- or heterodimers to consensus ATF/CRE sites in gene promoters to regulate transcription [8]. Like other members, full-length Atf3 possesses a basic region-leucine zipper (bZIP) domain for dimerization, although alternative splicing can produce Atf3 isoforms without a bZIP domain. The activity of some ATF/CREB proteins is regulated by phosphorylation, but Atf3 is largely regulated at the level of expression, being present at very low levels in quiescent cells and induced as an IEG by a range of extracellular stimuli (e.g. peptide growth factors, GqPCR agonists, cytokines) and cellular stresses (e.g. oxidative stress, ischaemia/reperfusion) in a variety of cell types. Indeed, it is difficult to identify a stimulus that does not induce Atf3 expression suggesting that it plays a significant, global role in regulating gene expression programmes. Mitogen-activated protein kinases (MAPKs) including ERK1/2 are particularly implicated in promoting Atf3 mRNA expression, potentially acting through a variety of transcription factors (e.g. CREB, Atf2, c-Myc) [9-11]. Several studies also implicate the Egr1 transcription factor in positive regulation of Atf3 transcription, probably resulting from its phosphorylation and activation by ERK1/2 [10,12,13].

Atf3 is generally viewed as a transcriptional repressor, particularly when present as homodimers. Thus, Atf3 represses transcription of Gadd153/Chop10 and may also repress transcription from its own promoter to limit expression [14]. A systems biology study of TLR4 signalling to gene expression in macrophages further confirmed its role as a transcriptional repressor, demonstrating that Atf3 is induced by lipopolysaccharide and represses expression of interleukin 6 (IL6) and IL12b mRNAs by antagonising NFκB-dependent stimulation of transcription [15]. A similar system operates downstream from TLR9 [16], suggesting that negative feedback regulation of cytokine production by Atf3 is a feature of the innate immune response [17]. However, Atf3 (potentially as heterodimers with other ATF/CREB proteins) promotes transcription of other genes such as proglucagon [18]. Moreover, in the context of DNA damage in cancer cells, Atf3 may act as a positive regulator of gene expression, probably by enhancing p53 function [19]. The dichotomous role of Atf3 and the variation in underlying mutations that cause cancer presumably account for the variation in opinion regarding the role of Atf3 in this disease [17].

As mentioned above, Atf3 is induced in cardiomyocytes by ET-1 as an IEG [5], but it is also upregulated in these cells by, for example, doxorubicin [20], oxidative stress [3], insulin [21] and hypoxia [22]. Transient ischaemia increases Atf3 expression in whole hearts

[22,23], and cardiospecific overexpression of Atf3 in transgenic mice results in pathological features of cardiac hypertrophy/failure [24] (this is distinguishable from, though may encompass, cardiomyocyte hypertrophy [25]). Confusingly, cardiac hypertrophy/failure induced by pressure-overload is exaggerated in Atf3 null mice [26]. This probably results from enhanced signalling through ERK1/2 and other MAPKs, all of which are implicated in the development of cardiac pathology [1]. Whilst these studies suggest that control of Atf3 expression is important in homeostatic control of cardiac function, it is difficult to develop a mechanistic understanding of Atf3 function in these models with long-term manipulation of Atf3 expression. We used the cardiomyocyte model to investigate the role of Atf3 in negative feedback regulation of IEG expression and positive feedforward regulation of second-phase genes. Adopting an antisense knockdown approach, we identified Egr1 as a prime target for Atf3 repression in response to ET-1. Notably, Egr1 has been associated with cardiac hypertrophy for many years [27-29], and our data shed further light on the transcriptional networks within which it operates.

EXPERIMENTAL

Cardiomyocyte cultures and knockdown of Atf3 with adenoviruses for antisense Atf3

Ventricles from neonatal Sprague-Dawley rat hearts (Harlan UK Ltd) were dissociated by serial digestion and cultured as previously described [6]. For immunoblotting, RNA studies or ChIP, cardiomyocytes were plated in 15% (v/v) foetal calf serum at a density of 4×10^6 cells/dish on 60 mm Primaria dishes pre-coated with sterile 1% (w/v) gelatin (Sigma-Aldrich UK). For immunostaining experiments, glass coverslips were placed in Primaria 35 mm culture dishes and coated with 1% (v/v) gelatin then laminin (0.2 mg/ml in PBS, 2 h). Coverslips were washed with PBS. Cardiomyocytes were plated at 1.5×10^6 cells/dish in serum-containing medium. After 18 h, cardiomyocytes were incubated in serum-free medium for 24 h then unstimulated (controls) or exposed to 100 nM ET-1 (Bachem UK) in the presence or absence of cycloheximide (Sigma-Aldrich UK), U0126 or PD184352 (Alexis Biochemicals, Enzo Life Sciences). Agonists/inhibitors were prepared as 1000× stock solutions in water (ET-1, cycloheximide) or DMSO (U0126, PD184352) and added directly to the tissue culture medium.

Preparation of adenoviruses

Replication-deficient AdVs expressing full-length rat Atf3 antisense RNA (AS-Atf3) were prepared using the AdEasy™ XL Adenoviral Vector System (Stratagene). The coding sequence for Atf3 was isolated by PCR from rat cardiomyocyte cDNA using Pfu polymerase and primers designed to the 5' start site (5'-ATGATGCTTCAACATCCAGGC-3') and 3' stop codon (5'-TTAGCTCTGCAATGTTCTTC-3') regions, and further amplified with primers that included sites for restriction enzymes HindIII (5'-CTTATCTAGAAGCTTATGATGCTTCAACATCCAGGC-3') and KpnI (5'-TAGAGATCTGGTACCTTAGCTCTGCAATGTTCTTC-3') for insertion into the multiple cloning site of the pShuttle-CMV vector. Control samples were prepared with empty vector (No-AS). Constructs were sequenced using an ABI 3100 Genetic Analyser. Shuttle plasmids were linearised with PmeI and used to transform BJ5183-AD-1 cells. AdV plasmids from positive recombinants were expanded in XL10Gold cells, linearised with PacI and used to transform HEK293 cells. AdVs were amplified through subsequent re-infection of HEK293

cells and titres were determined using Adeno-X™ Rapid Titer kits (Clontech). For experiments with AdVs, cardiomyocytes were incubated in serum-free medium for 4 h, AdVs were added and the cells incubated for a further 48 h.

Immunoblotting

Cardiomyocytes were washed in ice-cold PBS and nuclear extracts prepared for immunoblotting as described [30]. Proteins (20 µg) were separated by SDS-polyacrylamide gel electrophoresis on 10% or 12% polyacrylamide gels and transferred electrophoretically to nitrocellulose. Immunoblotting was performed as described [5]. Primary antibodies to Atf3 (sc-188), Egr1 (sc-189) and Atf2 (sc-187) were from Santa Cruz Biotechnology Inc. and used at 1/1000 dilution. Secondary antibodies conjugated to horseradish peroxidase were from Dako (1/5000 dilution). Bands were detected using ECL Plus with an ImageQuant 350 digital imager (GE Healthcare). ImageQuant 7.0 software was used for densitometric analysis.

RNA preparation, microarrays and data analysis

Cardiomyocytes were uninfected or infected with empty AdVs or AdVs encoding AS-Atf3 and then unstimulated (controls) or exposed to 100 nM ET-1 (90 min). Uninfected cardiomyocytes were exposed to ET-1 for 30, 60 or 90 min. Total RNA was prepared and concentrations determined as previously described [5]. To minimise variation resulting from different cardiomyocyte preparations, equal amounts of RNA from three individual experiments were pooled to generate a single sample set. Three sets of pooled samples were prepared for hybridization to separate Affymetrix rat exon 1.0 ST arrays (i.e. three separate sets of samples were analysed for each condition, prepared from a total of 9 myocyte preparations). Samples were prepared for hybridisation using Genechip® WT Sense Target Labelling kits (Affymetrix). For all samples except those from uninfected cells exposed to ET-1 for 60 min with their corresponding controls, the rRNA reduction protocol was modified and the RiboMinus Transcriptome Isolation Kit (Human/Mouse) (Invitrogen) was used according to the manufacturer's instructions with 7 µg of RNA. Hybridization to Affymetrix rat exon 1.0 ST arrays was performed at the CSC/IC Microarray Centre (Imperial College London). For samples from uninfected cells exposed to ET-1 for 60 min with their corresponding controls, total RNA was provided to the European Arabidopsis Stock Centre at Nottingham (NASC) for preparation and hybridisation to Affymetrix rat Exon 1.0 arrays according to their protocols (affymetrix.arabidopsis.info). Data are available from ArrayExpress (accession nos. E-MEXP-3392, E-MEXP-3393, E-MEXP-3394).

Data (.CEL files) were imported into GeneSpring 11.5 (Agilent Technologies) using the Extended annotations, with RMA16 normalisation and normalisation per gene to corresponding uninfected, unstimulated controls within each sample set. Probesets were selected for analysis with baseline expression >50 in all of any of the conditions. To determine effects of AdV infection, probesets were selected with >1.5-fold change in unstimulated cells infected with No-AS AdVs relative to uninfected cells, applying an unpaired T test with the Benjamini and Hochberg multiple testing correction (FDR<0.05). To identify transcripts regulated by Atf3, we selected those which were significantly changed (>1.5-fold; FDR<0.05) in uninfected cells in response to ET-1 at 30, 60 or 90 min (unpaired T-tests with the Benjamini and Hochberg multiple testing correction). For transcripts with <1.2-fold change in baseline expression with No-AS AdVs, subsequent analysis employed an

interpretation with AdV infected conditions, using statistical testing (one-way ANOVA with SNK post-test and Benjamini and Hochberg multiple testing correction) and filtering on the basis of >1.5-fold difference between AS-Atf3 and No-AS infected cells. For transcripts with >1.2-fold change in baseline expression with No-AS AdVs, subsequent analysis employed an interpretation with all conditions, using statistical testing (one-way ANOVA with SNK post-test and the Benjamini and Hochberg multiple testing correction) to identify mRNAs with significant difference between cells infected with AS-Atf3 and No-AS AdVs or uninfected cells, but with no significant difference between uninfected cells and those infected with No-AS AdVs with exposure to ET-1 (90 min) and/or in unstimulated cells. Further filtering identified transcripts with >1.5-fold difference between cells infected with AS-Atf3 and those infected with No-AS AdVs or uninfected cells.

PCR

Cardiomyocytes were treated and total RNA extracted as for microarray analysis. cDNAs were synthesized using High Capacity cDNA Reverse Transcription Kits with random primers (Applied Biosystems). Semi-quantitative PCR (sqPCR) and quantitative qPCR were performed as previously described [5] using primers listed in the Supplemental Information, Table 6 online. Values were normalized to glyceraldehyde 3-phosphate dehydrogenase (Gapdh) expression and then to control values.

Chromatin immunoprecipitation

Cardiomyocytes (16×10^6 cells per sample) were unstimulated or exposed to 100 nM ET-1 and fixed in 1% (v/v) formaldehyde (10 min). The reaction was terminated with 125 mM glycine (10 min). Cells were washed and harvested in ice-cold PBS containing protease/phosphatase inhibitors [5], collected by centrifugation ($3000 \times g$, 4°C, 5 min) and lysed (15 min, 4°C) in 50 mM Tris-HCl pH 8.0, 2 mM EDTA, 0.1% (v/v) Nonidet P40, 10% (v/v) glycerol containing protease/phosphatase inhibitors. Nuclei were pelleted ($3000 \times g$, 4°C, 5 min), resuspended in 50 mM Tris-HCl pH 8.0, 1% (w/v) SDS, 5 mM EDTA, and the DNA sheared to 200 - 800 bp fragments by sonication (5×30 s with 2 min recovery, 4°C). Following centrifugation ($4000 \times g$, 4°C, 5 min), the supernatants were retained and a sample reserved for input DNA. The remainder was diluted in 50 mM Tris-HCl pH 8.0, 0.5% (v/v) Nonidet P40, 200 mM NaCl, 0.5 mM EDTA. Samples were pre-cleared with protein A-Sepharose then incubated without or with 0.01 mg Atf3 antibodies (Santa Cruz Biotechnology Inc.; catalogue number, sc-188X) with rotation (4°C, overnight). Protein A-Sepharose was added together with sonicated salmon sperm DNA (1 µg/ml) and samples were incubated (4°C, 2 h). Beads were pelleted by centrifugation ($1000 \times g$, 4°C, 3 min) and washed (4°C, 3 min) in 20 mM Tris-HCl pH 8.0, 0.1% (w/v) SDS, 1% (v/v) Nonidet P40, 2 mM EDTA, 500 mM NaCl followed by 10 mM Tris-HCl pH 8.0 containing 1 mM EDTA. Immune complexes were eluted (10 min, 65°C) in 10 mM Tris-HCl pH 8.0, 1 mM EDTA, 1% (w/v) SDS. Samples were centrifuged ($200 \times g$, 1 min) and supernatants collected. Crosslinks were reversed by incubation (65°C, overnight) with 0.2 M NaCl. Samples were incubated (5 min, 4°C) with phenol:chloroform:isoamyl alcohol (25:24:1, pH 8.0) and the phases separated by centrifugation ($15,300 \times g$, 4°C, 10 min). DNA in the upper aqueous phase was precipitated with isopropanol (-80°C, 3 h), recovered by centrifugation ($15,300 \times g$, 10 min, 4°C), washed (70% (v/v) ethanol) and resuspended in nuclease free water for PCR. PCR reactions were performed using specific primers: Egr1, Forward 5'

ACTGCCGCTGTTCCAATACT 3', Egr1 Reverse 5' CGAATCGGCCTCTATTTCAA 3'; Ptgs2, Forward 5' GCAGCAAGCACGTCAGACT 3', Ptgs2 Reverse 5' TAACCCGGAGAACCTTGCTT 3'; IL6, Forward 5' TGCTCAAGTGCTGAGTCACT 3', IL6 Reverse 5' AGACTCATGGGAAAATCCCA 3'. Primers for an arbitrary downstream sequence ~2000 bp 3' to the IL6 promoter: Forward 5' CACCTCTCCACCCTGACATT 3', Reverse 5' CCAACTAGACAGCCCAGAGC 3'. PCR amplification conditions were: 34 cycles denaturing, 95°C, 30 s; annealing, 60°C, 30 s; extension 72°C, 45 s. PCR products were visualized on 2% (w/v) agarose gels with Sybr-Safe (Invitrogen) and the bands captured under UV illumination. Densitometric analysis was performed using Imagemaster 1D Prime, version 3.0 (GE Healthcare).

Immunostaining

Cardiomyocytes were exposed to 100 nM ET-1, then washed with PBS and fixed in 4% (v/v) formaldehyde (10 min, room temperature). Immunostaining was performed as described previously [31] using mouse monoclonal primary antibodies to troponin T (1/40, 60 min; Stratech Scientific, catalogue no. MS-295-P1) and Alexa Fluor®488 anti-mouse secondary antibodies (1/200, 60 min). Coverslips were mounted using fluorescent mounting medium (Dako) and viewed using a Zeiss Axioskop fluorescence microscope. Images were captured using a digital camera (1600 × 1200 pixels resolution, 1.4× zoom factor, 160 × 120 µm field dimension). Colour images were converted to Greyscale using Adobe Photoshop.

Statistical analysis

Statistical analysis of microarray data used GeneSpring 11.5. Other analyses used GraphPad Prism 4.0.

RESULTS

Regulation of Atf3 expression in cardiomyocytes by ET-1 and identification of Atf3 target genes

ET-1 (100 nM) stimulated a rapid, transient increase in expression of Atf3 mRNA in cardiomyocytes (Figure 1A). Expression was maximal within 30 min, declining rapidly thereafter. Cycloheximide (a protein synthesis inhibitor) did not inhibit the response, indicating that Atf3 was regulated as an IEG (Figure 1B), and upregulation of Atf3 mRNA by ET-1 was inhibited by U0126 or PD184352, inhibitors of the ERK1/2 cascade (Figure 1, B and C). Atf3 protein was also increased by ET-1 (maximal at 1 h) (Figure 1D). To suppress expression of Atf3, we generated adenoviruses (AdVs) encoding full-length Atf3 in the antisense orientation (AS-Atf3), using empty AdVs with no AS-Atf3 (No-AS) to control for effects of viral infection. Effective knockdown of Atf3 protein induced by ET-1 was obtained using 150 MOI AS-Atf3 AdVs with limited effect of No-AS AdVs and no effect on expression of Atf2 (Figure 1, E-G).

Uninfected cardiomyocytes or cardiomyocytes infected with 150 MOI No-AS or AS-Atf3 AdVs were unstimulated or exposed to 100 nM ET-1 for 90 min (since expression of Atf3 protein was maximal at 1 h, Figure 1D, we expected to detect downstream consequences by 90 min) and mRNA expression profiling was performed (Affymetrix rat exon 1.0 ST

microarrays). As expected, No-AS AdV infection alone significantly (>1.5 -fold; $\text{FDR} < 0.05$) affected expression of a subset of mRNAs (156 mRNAs upregulated; 59 mRNAs downregulated), many of which are associated with a viral response and/or cytokine/chemokine signalling in other cells (Figure 2; Supplemental Information, Table 1).

To determine the effects of Atf3 in the ET-1-responsive myocyte transcriptome, probesets were selected with significant changes in expression (>1.5 -fold, $\text{FDR} < 0.05$) induced by ET-1 at 30, 60, or 90 min (334 upregulated and 109 downregulated mRNAs). From these, we identified 90 mRNAs that were upregulated by ET-1 and affected by Atf3 knockdown (Figure 3A; Supplemental Information, Tables 2 - 4 online). Of upregulated transcripts without baseline effect of viral infection (75 mRNAs), AS-Atf3 enhanced the response of 15 mRNAs (clusters A1 and A2), inhibited the response of 18 mRNAs (clusters B1 and B2) and, for 42 mRNAs (cluster C), AS-Atf3 enhanced the response in unstimulated cells without further effect on the response to ET-1. Of upregulated mRNAs with baseline (>1.2 -fold change) effect of viral infection, the response to ET-1 was enhanced or inhibited by AS-Atf3 for 8 (cluster D) or 7 (cluster E) mRNAs, respectively. With ET-1 downregulated mRNAs (Figure 3B; Supplemental Information, Table 5 online), we identified only 5 mRNAs for which AS-Atf3 reduced the magnitude of the downregulation by ET-1 (cluster F) and 5 mRNAs for which AS-Atf3 increased the magnitude of the response (cluster G). Having previously defined IEG vs downstream gene expression for mRNAs upregulated by ET-1 (Affymetrix rat genome 230 2.0 arrays) [5], we cross-referenced the datasets (Supplemental Information, Tables 2 and 4 online). A greater proportion of mRNAs in clusters A1, A2 and D (Atf3 knockdown enhanced ET-1-induced expression) were IEGs rather than second-phase genes, consistent with negative feedback by Atf3. A greater proportion of mRNAs in clusters B1 and B2 (Atf3 knockdown inhibited ET-1-induced expression) were second-phase genes rather than IEGs suggesting that Atf3 plays a positive feed-forward role in these cases (genes in cluster E were not identified in the previous dataset [5]). Overall, we conclude that upregulation of Atf3 by ET-1 in cardiomyocytes plays a significant role in modulating the response of other upregulated genes, and a minor role in regulating mRNAs that are downregulated by ET-1.

Negative regulation of Egr1 and Ptgs2 expression by Atf3

Microarray data were validated by qPCR, selecting IEGs with enhanced expression of the ET-1 response by AS-Atf3 (Egr1, Ptgs2) and non-IEGs with reduced expression by AS-Atf3 (Areg, Dusp5) for analysis. For Egr1 and Ptgs2, the relative increase in expression induced by ET-1 at 0.5 h was similar in cardiomyocytes expressing No-AS or AS-Atf3 (Figure 4, A and B), indicating that Atf3 was not involved in this upregulation phase. AS-Atf3 produced sustained expression of Egr1 mRNA (Figure 4A) and enhanced expression of Ptgs2 at subsequent times (Figure 4B), consistent with negative feedback of Atf3 on these two genes. In contrast, AS-Atf3 inhibited expression of Areg (Figure 4C) and Dusp5 (Figure 4D). The qPCR data (Figure 4, left panels) are consistent with the microarray results (Figure 4, right panels). Dusp1 (an IEG) and Il1rl1 (a non-IEG) were not significantly affected by AS-Atf3 in our microarray experiments and there was no difference in the relative changes in expression induced by ET-1 in cardiomyocytes expressing No-AS or AS-Atf3 (Figure 4, E and F). Thus, our selection criteria were not excessively stringent. Finally, although others identified IL6 as a target for negative feedback by Atf3 in the context of inflammation [15], there was no difference in relative expression of IL6 mRNA in cardiomyocytes expressing No-AS or AS-Atf3 following stimulation with ET-1 at any time studied (Figure 4G). To validate the Atf3-Egr1 feedback loop further, we examined the effect of AS-Atf3 on Egr1

protein expression following induction with ET-1. AS-Atf3 (but not No-AS) inhibited expression of Atf3 for the 150 min period studied (Figure 5, A and B). AS-Atf3 did not substantially increase the total amount of Egr1 protein at 60 min, but levels remained elevated up to ~105 min (Figure 5, A and C). After this time Egr1 protein declined, but levels remained elevated up to at least 150 min.

Chromatin immunoprecipitation (ChIP) with antibodies to Atf3 was used to determine if Atf3 binds directly to the Egr1 and Ptgs2 promoters. The Egr1 promoter contains two CRE elements [32], and a CRE-element potentially subject to negative regulation by Atf3 has been identified in the Ptgs2 promoter [33,34]. We used primers either side of these sequences for ChIP-PCR (Figure 6, A and C). For both genes, the amount of ChIP-PCR product in unstimulated cells was similar to that of no-antibody controls and stimulation with ET-1 (1 h) substantially increased the amount of ChIP-PCR product (Figure 6, B and D). Thus, Atf3 binds directly to Egr1 and Ptgs2 promoters to inhibit transcription. Interestingly, ChIP-PCR for the IL6 promoter (Figure 6E) demonstrated binding of Atf3 (Figure 6F) despite there being no effect of Atf3 knockdown on expression of IL6 mRNA (Figure 4G). This is discussed below, but potentially results from ET-1 signalling through ERK1/2 rather than NF κ B. The specificity of the ChIP-PCR experiments was demonstrated by PCR across an arbitrary sequence approximately 2000 bp downstream of the IL6 promoter (Figure 6G).

Mathematical modelling of the Atf3-Egr1 negative feedback loop

Atf3 appears to be a dominant negative regulatory factor in suppressing Egr1 transcription (Figure 4A), but we cannot eliminate the possibility of additional negative regulatory elements from the experimental data. We therefore developed a deterministic ordinary differential equation model for the Atf3-Egr1 feedback system (Figure 7A) to determine whether Atf3 expression can suffice to suppress Egr1 transcription. We assumed the following: Atf3 and Egr1 are co-regulated through ERK1/2 signalling (expression of each requires a similar degree of ERK1/2 signalling [5]); ERK1/2 promote expression by increasing transactivating activities of transcription factors pre-bound to both promoters (i.e. the transcription factor/promoter is viewed as a single entity regulated by ERK1/2 binding/phosphorylation); it was not necessary to consider ERK1/2 or Atf3 signal termination (i.e. no attempt was made to switch off the signal). The model was informed initially by parameters derived in this study and from published literature (Supplemental Information, Mathematical Modelling online).

We initially assumed that Atf3 suppression of Egr1 mRNA transcription was competitive with the positive ERK1/2 signal, but this did not give a good fit to the experimental data. An alternative model in which Atf3 eliminates the ERK1/2 signal (modelled by removing the ERK1/2 signal upon Atf3 binding, Figure 7A) gave a good qualitative fit. Adjusting the rate of mRNA synthesis to 275 b/s (within the recently estimated range of 55 to >800 b/s [35,36]) for calculation of the rates of transcription of Egr1 and Atf3 mRNAs, and adjusting parameters for association of phosphorylated ERK1/2 with Egr1 and Atf3 DNA (see Supplemental Information, Mathematical Modelling online) gave a very good fit to the experimental data in terms of magnitude of variation in Egr1 mRNA (~20-fold, Figure 4A), and a relatively good fit (qualitatively) to the suppression of Egr1 mRNA by Atf3. The best fit model was obtained with a rate of Atf3 suppression of Egr1 transcription (k_7) in the range $1 \times 10^5(\text{Ms})^{-1} \leq k_7 \leq 6 \times 10^5(\text{Ms})^{-1}$ (Figure 7B). Modelling the system in the absence of Atf3 (to mimic Atf3 knockdown) resulted in a similar rate of production of Egr1 mRNA to ~0.5 h, with sustained expression thereafter (Figure 7B, centre left panel), a profile that replicates the experimental data (Figure 4A, left panel). Thus, Atf3

alone can account for the suppression of Egr1 mRNA expression and probably does so by over-riding the positive ERK1/2 signal.

Effects of Atf3 on morphological changes induced in cardiomyocytes by ET-1

To determine the consequences of knockdown of Atf3 for ET-1-induced hypertrophy, we examined the effects of AS-Atf3 AdVs on myocyte morphology by immunostaining for troponin T, a component of the myofibrillar apparatus. As shown previously [37,38], uninfected and unstimulated cardiomyocytes appear small with disorganised myofilaments (Figure 8A). Stimulation with ET-1 increased cell size, increased the content/organisation of myofilaments and promoted formation of cell-cell contacts (Figure 8B), classic features of hypertrophy. No-AS AdVs increased myofibrillar content to a small degree in unstimulated cells (Figure 8C), but had no overt effect on morphological changes induced by ET-1 (Figure 8D). Relative to No-AS AdVs, AS-Atf3 AdVs had no effect on unstimulated cells, but resulted in abnormal morphology following ET-1 stimulation with "clumping" of cells and generation of elongated processes extending between them (Figure 8, E - H). It is unclear if this is an effect on hypertrophy *per se* or whether there is a loss of cell-cell or cell-matrix adhesion. Thus, although Atf3 is transiently upregulated within the first hour of stimulation, it has a significant effect on long-term phenotypic changes.

Discussion

Atf3 is emerging as an extremely important feedback regulator of transcription in general. Greatest emphasis has been placed on its role in inflammation and it is clear that Atf3 is essential for restraining the immune response [15,17]. However, although viewed as a stress-regulated and stress-regulatory gene, Atf3 is also upregulated in many cells by growth stimuli including peptide growth factors and GqPCR agonists [5,39-41]. The genes that Atf3 regulates in a growth context are likely to differ from those that it regulates in a stress response. Here, we identify a number of genes that are regulated in cardiomyocytes in response to ET-1 for which Atf3 plays either a negative feedback or positive feedforward role (Figure 3). Since loss of Atf3 results in a severely abnormal response to ET-1 (Figure 8), strict regulation of any or all of these targets must be important in ensuring an appropriate hypertrophic growth response. However, of all the potential targets, Egr1 emerged as a significant candidate and we provide substantial evidence that Atf3 is a transcriptional repressor for Egr1 in the ET-1 response. Thus, Atf3 knockdown leads to sustained expression of Egr1 mRNA and enhanced expression of Egr1 protein, and Atf3 binds directly to the Egr1 promoter. Furthermore, mathematical modelling of the system established that Atf3 alone can suffice to suppress Egr1 mRNA expression.

Egr1 was among the first IEGs to be identified [42] and it is upregulated in many cells in response to a wide range of growth stimuli [43]. As such, it is implicated in a host of different systems including kidney differentiation [44], macrophage differentiation [45], the nervous system and learning/memory [46,47], the immune response [48], wound healing and tissue repair [49], prostate cancer [50] and acute lung injury [51]. In the vascular system, Egr1 is associated with excessive smooth muscle cell proliferation resulting in in-stent restenosis following angioplasty [52]. Egr1 is also implicated in cardiac/cardiomyocyte hypertrophy. Thus, expression of Egr1 is increased in cardiomyocytes and the heart in response to a variety of hypertrophic stimuli [27,28], and loss of Egr1 attenuates the hypertrophic response [29]. The importance of Egr1 in such a range of systems, together

with the emergence of Atf3 as a negative feedback regulator and the co-regulation of the two genes in many situations, raises the possibility that the Atf3→Egr1 negative feedback loop is of broad general significance required to restrict expression of Egr1 and maintain a normal growth response.

Although Atf3 and Egr1 are co-regulated by a range of stimuli, their upregulation is usually rapid and transient. As transcription factors, IEGs such as Atf3 and Egr1 are important in regulating downstream gene expression and dysregulation leads to functional abnormalities and abnormal phenotypic responses. As we demonstrated (Figure 8), cardiomyocyte hypertrophy cannot proceed normally in the absence of Atf3. This is not inconsistent with induction of cardiac hypertrophy in mice *in vivo* by overexpression of Atf3 [24]. Atf3 knockout also enhances cardiac hypertrophy induced by pressure-overload in mice but, in this model, MAPK signalling (including ERK1/2) induced by pressure-overload is significantly enhanced [19] and this alone could account for enhanced hypertrophy [2,53]. Intriguing questions relate to how Atf3 modulates MAPK signalling and if the upregulation of MAPK signalling is a compensatory mechanism for loss of Atf3. Other studies indicate that Atf3 is important in regulating, for example, the immune response [15,17], liver function [54] and pancreatic β -cell function [55,56]. Because of this, it is important to identify the genes that Atf3 regulates.

At least two previous studies took a systems approach to identify Atf3-regulated genes, neither of which identified Egr1 as a target. The first focused on TLR4 signalling and the effects of lipopolysaccharide on the macrophage transcriptome [15]. The strategy used Cytoscape (software that draws on published literature to identify protein-protein interactions) to predict Atf3-regulated genes from microarray data for subsequent experimental verification. Atf3 was particularly implicated in negative regulation of IL6. IL6 is upregulated in cardiomyocytes by ET-1 as we have previously reported [57] and as we show in this study (Figure 4G). We also previously reported preliminary data on the effects of AS-Atf3 AdV infection on IL6 mRNA expression. In those experiments, low viral titres and a low MOI (<15) were used to suppress the increase in expression of Atf3 by 10 nM ET-1 (rather than 100 nM ET-1 used here). As in this study, AS-Atf3 AdVs enhanced the increase in IL6 mRNA induced by ET-1 [57]. Our interpretation was that Atf3 suppressed IL6 transcription, consistent with the report on the role of Atf3 in the TLR4 response [15]. However, we know now that AdV infection has substantial effects on elements of the cardiomyocyte transcriptome and on IL6 in particular (Figure 2), and the data in the earlier report require re-interpretation. With submaximal virus and agonist concentrations (rather than the saturation levels used in this study), slight differences between No-AS and AS-Atf3 viral titres were likely to be exaggerated. The No-AS AdV titre may have been slightly less than that of the AS-Atf3 AdVs and this could account for the significant effect of AS-Atf3 on IL6 mRNA expression in control cells over and above that induced by the empty virus. We assumed that this indicated a basal effect of Atf3 on IL6 mRNA expression. However, if the effect of AS-Atf3 in control cells is taken into account, ET-1 stimulation of IL6 mRNA was similar (~4-fold) in cardiomyocytes infected with either No-AS or AS-Atf3 AdVs. We now therefore consider that Atf3 knockdown did not influence the increase in expression of IL6 mRNA induced by ET-1. The lack of an effect of Atf3 knockdown on the increase in IL6 mRNA expression induced by ET-1 in contrast to the TLR4 response probably reflects a fundamental difference in the signalling mechanisms. TLR4 signals predominantly through NF κ B and suppression of IL6 expression by Atf3 results from its interaction with and inhibition of NF κ B [15]. ET-1 signals predominantly through ERK1/2 to upregulate expression of IL6 [5]. With little/no signal through NF κ B, Atf3 is unlikely to inhibit transcription of IL6. However, Atf3 still binds to the IL6 promoter (Figure 6G). It is less clear why Egr1 was not identified as an Atf3-regulated gene in the TLR4 study [15]. One

reason may be that Cytoscape is informed only by published data. Hence, the study focused on the Atf3/NFκB interaction and all validations centred on the NFκB response.

The second study identifying Atf3-regulated genes focused on DNA damage in cancer cells. Here, 5,984 potential Atf3-binding promoters were identified in HCT116 colon cancer cells subjected to DNA damage and 1,493 were identified in LNCaP prostate cancer cells exhibiting enhanced Atf3 expression [19]. In contrast to TLR4 signalling in macrophages [15], Atf3 plays a greater role in positive regulation of mRNA expression in these cancer cells, and there was no obvious effect of Atf3 knockdown on Egr1 expression. However, this paradigm differs radically from a growth response associated with IEG expression: Atf3 upregulation is delayed (mRNA and protein expression are maximal at 6 and 12 h, respectively) and potentially driven by p53 [58] with many of the Atf3-regulated genes being classic p53 targets [19]. It should also be considered that cancer cell lines were used rather than primary cells, and this may influence the signalling/gene expression response.

Since Atf3 and Egr1 are co-regulated in many systems, it is worth considering the extent to which the Atf3-Egr1 feedback mechanism operates. We expect it will apply in cardiomyocytes exposed to other stimuli that regulate gene expression primarily through MAPK signalling. We suggest that the Atf3-Egr1 negative feedback loop operates in other systems that also drive gene expression primarily through ERK1/2 signalling, but this awaits further investigation.

AUTHOR CONTRIBUTION

The study was conceived and directed by Angela Clerk. Alejandro Giraldo and Oliver P.T Barrett conducted the majority of the experimental work, with equal contribution. Stephen J. Fuller constructed the vectors, produced the AdVs for this study and, with Emre Amirak, assisted with parameterisation of the model. Emre Amirak contributed microarray data and performed qPCR experiments. The mathematical modelling was performed by Marcus J. Tindall with assistance from Bonhi S. Bhattacharya. Overall supervision of the study was undertaken by Angela Clerk and Peter H. Sugden.

FUNDING AND ACKNOWLEDGEMENTS

This study was funded by the British Heart Foundation (grant PG/07/074/23445) and Fondation Leducq (Transatlantic Network of Excellence grant CV05-02). We wish to thank Ross Bullivant and Joel Pearson for assistance in the initial phase of the mathematical modelling. Mr. Bullivant was funded by a Nuffield undergraduate research bursary. Mr. Pearson was funded by the University of Reading Undergraduate Research Opportunities scheme.

REFERENCES

- 1 Sugden, P. H. and Clerk, A. (1998) Cellular mechanisms of cardiac hypertrophy. *J.Mol.Med.* **76**, 725-746
- 2 Heineke, J. and Molkentin, J. D. (2006) Regulation of cardiac hypertrophy by intracellular signalling pathways. *Nat.Rev.Mol.Cell Biol.* **7**, 589-600

- 3 Clerk, A., Kemp, T. J., Zoumpoulidou, G., and Sugden, P. H. (2007) Cardiac myocyte gene expression profiling during H₂O₂-induced apoptosis. *Physiol.Genomics* **29**, 118-127
- 4 Kennedy, R. A., Kemp, T. J., Sugden, P. H., and Clerk, A. (2006) Using U0126 to dissect the role of the extracellular signal-regulated kinase 1/2 (ERK1/2) cascade in the regulation of gene expression by endothelin-1 in cardiac myocytes. *J.Mol.Cell.Cardiol.* **41**, 236-247
- 5 Cullingford, T. E., Markou, T., Fuller, S. J., Giraldo, A., Pikkarainen, S., Zoumpoulidou, G., Alsafi, A., Ekere, C., Kemp, T. J., Dennis, J. L., Game, L., Sugden, P. H., and Clerk, A. (2008) Temporal regulation of expression of immediate early and second phase transcripts by endothelin-1 in cardiomyocytes. *Genome Biol.* **9**, R32
- 6 Marshall, A. K., Barrett, O. P., Cullingford, T. E., Shanmugasundram, A., Sugden, P. H., and Clerk, A. (2010) ERK1/2 signaling dominates over RhoA signaling in regulating early changes in RNA expression induced by endothelin-1 in neonatal rat cardiomyocytes. *PLoS One* **5**, e10027
- 7 Clerk, A., Gillespie-Brown, J., Fuller, S. J., and Sugden, P. H. (1996) Stimulation of phosphatidylinositol hydrolysis, protein kinase C translocation, and mitogen-activated protein kinase activity by bradykinin in ventricular myocytes. Dissociation from the hypertrophic response. *Biochem.J.* **317**, 109-118
- 8 Hai, T. and Hartman, M. G. (2001) The molecular biology and nomenclature of the activating transcription factor/cAMP responsive element binding family of transcription factors: activating transcription factor proteins and homeostasis. *Gene* **273**, 1-11
- 9 Lu, D., Chen, J., and Hai, T. (2007) The regulation of ATF3 gene expression by mitogen-activated protein kinases. *Biochem.J.* **401**, 559-567
- 10 Mayer, S. I., Dexheimer, V., Nishida, E., Kitajima, S., and Thiel, G. (2008) Expression of the transcriptional repressor ATF3 in gonadotrophs is regulated by Egr-1, CREB, and ATF2 after gonadotropin-releasing hormone receptor stimulation. *Endocrinology* **149**, 6311-6325
- 11 Tamura, K., Hua, B., Adachi, S., Guney, I., Kawauchi, J., Morioka, M., Tamamori-Adachi, M., Tanaka, Y., Nakabeppu, Y., Sunamori, M., Sedivy, J. M., and Kitajima, S. (2005) Stress response gene ATF3 is a target of c-myc in serum-induced cell proliferation. *EMBO J.* **24**, 2590-2601
- 12 Yamaguchi, K., Lee, S. H., Kim, J. S., Wimalasena, J., Kitajima, S., and Baek, S. J. (2006) Activating transcription factor 3 and early growth response 1 are the novel targets of LY294002 in a phosphatidylinositol 3-kinase-independent pathway. *Cancer Res.* **66**, 2376-2384
- 13 Bottone, F. G., Moon, Y., Alston-Mills, B., and Eling, T. E. (2005) Transcriptional regulation of activating transcription factor 3 involves the early growth response-1 gene. *J.Pharmacol.Exp.Ther.* **315**, 668-677
- 14 Wolfgang, C. D., Liang, G., Okamoto, Y., Allen, A. E., and Hai, T. (2000) Transcriptional autorepression of the stress-inducible gene ATF3. *J.Biol.Chem.* **275**, 16865-16870
- 15 Gilchrist, M., Thorsson, V., Li, B., Rust, A. G., Korb, M., Kennedy, K., Hai, T., Bolouri, H., and Aderem, A. (2006) Systems biology approaches identify ATF3 as a negative regulator of Toll-like receptor 4. *Nature* **441**, 173-178
- 16 Whitmore, M. M., Iparraguirre, A., Kubelka, L., Weninger, W., Hai, T., and Williams, B. R. (2007) Negative regulation of TLR-signaling pathways by activating transcription factor-3. *J.Immunol.* **179**, 3622-3630
- 17 Thompson, M. R., Xu, D., and Williams, B. R. (2009) ATF3 transcription factor and its emerging roles in immunity and cancer. *J.Mol.Med.(Berl)* **87**, 1053-1060

- 18 Wang, J., Cao, Y., and Steiner, D. F. (2003) Regulation of proglucagon transcription by activated transcription factor (ATF) 3 and a novel isoform, ATF3b, through the cAMP-response element/ATF site of the proglucagon gene promoter. *J.Biol.Chem.* **278**, 32899-32904
- 19 Tanaka, Y., Nakamura, A., Morioka, M. S., Inoue, S., Tamamori-Adachi, M., Yamada, K., Taketani, K., Kawauchi, J., Tanaka-Okamoto, M., Miyoshi, J., Tanaka, H., and Kitajima, S. (2011) Systems analysis of ATF3 in stress response and cancer reveals opposing effects on pro-apoptotic genes in p53 Pathway. *PLoS One* **6**, e26848
- 20 Nobori, K., Ito, H., Tamamori-Adachi, M., Adachi, S., Ono, Y., Kawauchi, J., Kitajima, S., Marumo, F., and Isobe, M. (2002) ATF3 inhibits doxorubicin-induced apoptosis in cardiac myocytes: a novel cardioprotective role of ATF3. *J.Mol.Cell.Cardiol.* **34**, 1387-1397
- 21 Markou, T., Marshall, A. K., Cullingford, T. E., Tham, E. L., Sugden, P. H., and Clerk, A. (2010) Regulation of the cardiomyocyte transcriptome vs translome by endothelin-1 and insulin: translational regulation of 5' terminal oligopyrimidine tract (TOP) mRNAs by insulin. *BMC Genomics* **11**, 343
- 22 Kim, M. Y., Seo, E. J., Lee, D. H., Kim, E. J., Kim, H. S., Cho, H. Y., Chung, E. Y., Lee, S. H., Baik, E. J., Moon, C. H., and Jung, Y. S. (2010) Gadd45beta is a novel mediator of cardiomyocyte apoptosis induced by ischaemia/hypoxia. *Cardiovasc.Res.* **87**, 119-126
- 23 Liu, L., Zhu, J., Glass, P. S., Brink, P. R., Rampil, I. J., and Rebecchi, M. J. (2009) Age-associated changes in cardiac gene expression after preconditioning. *Anesthesiology* **111**, 1052-1064
- 24 Okamoto, Y., Chaves, A., Chen, J., Kelley, R., Jones, K., Weed, H. G., Gardner, K. L., Gangi, L., Yamaguchi, M., Klomkleaw, W., Nakayama, T., Hamlin, R. L., Carnes, C., Altschulk, R., Bauer, J., and Hai, T. (2001) Transgenic mice with cardiac-specific expression of activating transcription factor 3, a stress-inducible gene, have conduction abnormalities and contractile dysfunction. *Am.J.Pathol.* **159**, 639-650
- 25 Dorn, G. W., II, Robbins, J., and Sugden, P. H. (2003) Phenotyping hypertrophy: eschew obfuscation. *Circ.Res.* **92**, 1171-1175
- 26 Zhou, H., Shen, D. F., Bian, Z. Y., Zong, J., Deng, W., Zhang, Y., Guo, Y. Y., Li, H., and Tang, Q. Z. (2011) Activating transcription factor 3 deficiency promotes cardiac hypertrophy, dysfunction, and fibrosis induced by pressure overload. *PLoS One* **6**, e26744
- 27 Iwaki, K., Sukhatme, V. P., Shubeita, H. E., and Chien, K. R. (1990) α - and β -Adrenergic stimulation induces distinct patterns of immediate early gene expression in neonatal rat myocardial cells. *fos/jun* expression is associated with sarcomere assembly; *Egr-1* induction is primarily an α_1 -mediated response. *J.Biol.Chem.* **265**, 13809-13817
- 28 Neyses, L. and Pelzer, T. (1995) The biological cascade leading to cardiac hypertrophy. *Eur.Heart J.* **16 Suppl N**, 8-11
- 29 Saadane, N., Alpert, L., and Chalifour, L. E. (2000) Altered molecular response to adrenoreceptor-induced cardiac hypertrophy in *Egr-1*-deficient mice. *Am.J.Physiol Heart Circ.Physiol.* **278**, H796-H805
- 30 Clerk, A. and Sugden, P. H. (1997) Cell stress-induced phosphorylation of ATF2 and c-Jun transcription factors in rat ventricular myocytes. *Biochem.J.* **325**, 801-810
- 31 Sugden, P. H., Markou, T., Fuller, S. J., Tham, E. L., Molkentin, J. D., Paterson, H. F., and Clerk, A. (2011) Monophosphothreonyl extracellular signal-regulated kinases 1 and 2 (ERK1/2) are formed endogenously in intact cardiac myocytes and are enzymically active. *Cell.Signal.* **23**, 468-477

- 32 Meyer, R. G., Kupper, J. H., Kandolf, R., and Rodemann, H. P. (2002) Early growth response-1 gene (Egr-1) promoter induction by ionizing radiation in U87 malignant glioma cells in vitro. *Eur.J.Biochem.* **269**, 337-346
- 33 Xie, W., Fletcher, B. S., Andersen, R. D., and Herschman, H. R. (1994) v-src induction of the TIS10/PGS2 prostaglandin synthase gene is mediated by an ATF/CRE transcription response element. *Mol.Cell.Biol.* **14**, 6531-6539
- 34 Xie, W. and Herschman, H. R. (1995) v-src induces prostaglandin synthase 2 gene expression by activation of the c-Jun N-terminal kinase and the c-Jun transcription factor. *J.Biol.Chem.* **270**, 27622-27628
- 35 Ben-Ari, Y., Brody, Y., Kinor, N., Mor, A., Tsukamoto, T., Spector, D. L., Singer, R. H., and Shav-Tal, Y. (2010) The life of an mRNA in space and time. *J.Cell Sci.* **123**, 1761-1774
- 36 Maiuri, P., Knezevich, A., De, M. A., Mazza, D., Kula, A., McNally, J. G., and Marcello, A. (2011) Fast transcription rates of RNA polymerase II in human cells. *EMBO Rep.* **12**, 1280-1285
- 37 Clerk, A., Michael, A., and Sugden, P. H. (1998) Stimulation of the p38 mitogen-activated protein kinase pathway in neonatal rat ventricular myocytes by the G protein-coupled receptor agonists, endothelin-1 and phenylephrine: a role in cardiac myocyte hypertrophy? *J.Cell Biol.* **142**, 523-535
- 38 Clerk, A., Aggeli, I.-K. S., Stathopoulou, K., and Sugden, P. H. (2006) Peptide growth factors signal differentially through protein kinase C to extracellular signal-regulated kinases in neonatal cardiomyocytes. *Cell.Signal.* **18**, 225-235
- 39 Nagashima, T., Shimodaira, H., Ide, K., Nakakuki, T., Tani, Y., Takahashi, K., Yumoto, N., and Hatakeyama, M. (2007) Quantitative transcriptional control of ErbB receptor signaling undergoes graded to biphasic response for cell differentiation. *J.Biol.Chem.* **282**, 4045-4056
- 40 Uzonyi, B., Lotzer, K., Jahn, S., Kramer, C., Hildner, M., Bretschneider, E., Radke, D., Beer, M., Vollandt, R., Evans, J. F., Funk, C. D., and Habenicht, A. J. (2006) Cysteinyl leukotriene 2 receptor and protease-activated receptor 1 activate strongly correlated early genes in human endothelial cells. *Proc.Natl.Acad.Sci.U.S.A* **103**, 6326-6331
- 41 Schweighofer, B., Testori, J., Sturtzel, C., Sattler, S., Mayer, H., Wagner, O., Bilban, M., and Hofer, E. (2009) The VEGF-induced transcriptional response comprises gene clusters at the crossroad of angiogenesis and inflammation. *Thromb.Haemost.* **102**, 544-554
- 42 Sukhatme, V. P., Cao, X., Chang, L. C., Tsai-Morris, C., Stamenkovich, D., Ferreira, P. C. P., Cohen, D. R., Edwards, S. A., Shows, T. B., Curran, T., Le Beau, M. M., and Adamson, E. D. (1988) A zinc finger-encoding gene coregulated with *c-fos* during growth and differentiation, and after cellular depolarization. *Cell* **53**, 37-43
- 43 Sukhatme, V. P. (1990) Early transcriptional events in cell growth: the Egr family. *J.Am.Soc.Nephrol.* **1**, 859-866
- 44 Sukhatme, V. P. (1992) The Egr transcription factor family: from signal transduction to kidney differentiation. *Kidney Int.* **41**, 550-553
- 45 Liebermann, D. A. and Hoffman, B. (1994) Differentiation primary response genes and proto-oncogenes as positive and negative regulators of terminal hematopoietic cell differentiation. *Stem Cells* **12**, 352-369
- 46 Beckmann, A. M. and Wilce, P. A. (1997) Egr transcription factors in the nervous system. *Neurochem.Int.* **31**, 477-510
- 47 Walton, M., Henderson, C., Mason-Parker, S., Lawlor, P., Abraham, W. C., Bilkey, D., and Dragunow, M. (1999) Immediate early gene transcription and synaptic modulation. *J.Neurosci.Res.* **58**, 96-106

- 48 McMahon, S. B. and Monroe, J. G. (1996) The role of early growth response gene 1 (egr-1) in regulation of the immune response. *J.Leukoc.Biol.* **60**, 159-166
- 49 Braddock, M. (2001) The transcription factor Egr-1: a potential drug in wound healing and tissue repair. *Ann.Med.* **33**, 313-318
- 50 Adamson, E. D. and Mercola, D. (2002) Egr1 transcription factor: multiple roles in prostate tumor cell growth and survival. *Tumour Biol.* **23**, 93-102
- 51 Ngiam, N., Post, M., and Kavanagh, B. P. (2007) Early growth response factor-1 in acute lung injury. *Am.J.Physiol Lung Cell Mol.Physiol.* **293**, L1089-L1091
- 52 Khachigian, L. M. (2001) Catalytic oligonucleotides targeting EGR-1 as potential inhibitors of in-stent restenosis. *Ann.N.Y.Acad.Sci.* **947**, 412-415
- 53 Clerk, A., Cullingford, T. E., Fuller, S. J., Giraldo, A., Markou, T., Pikkarainen, S., and Sugden, P. H. (2007) Signaling pathways mediating cardiac myocyte gene expression in physiological and stress responses. *J.Cell.Physiol.* **212**, 311-322
- 54 Allen-Jennings, A. E., Hartman, M. G., Kociba, G. J., and Hai, T. (2002) The roles of ATF3 in liver dysfunction and the regulation of phosphoenolpyruvate carboxykinase gene expression. *J.Biol.Chem.* **277**, 20020-20025
- 55 Zmuda, E. J., Qi, L., Zhu, M. X., Mirmira, R. G., Montminy, M. R., and Hai, T. (2010) The roles of ATF3, an adaptive-response gene, in high-fat-diet-induced diabetes and pancreatic beta-cell dysfunction. *Mol.Endocrinol.* **24**, 1423-1433
- 56 Zmuda, E. J., Viapiano, M., Grey, S. T., Hadley, G., Garcia-Ocana, A., and Hai, T. (2010) Deficiency of Atf3, an adaptive-response gene, protects islets and ameliorates inflammation in a syngeneic mouse transplantation model. *Diabetologia* **53**, 1438-1450
- 57 Clerk, A., Cullingford, T.E., Fuller, S.J., Giraldo, A., and Sugden, P.H. (2009) Endothelin-1 regulation of immediate early gene expression in cardiac myocytes: negative feedback regulation of interleukin 6 by Atf3 and Klf2. *Adv.Enzyme Regul.* **49**, 30-42
- 58 Fan, F., Jin, S., Amundson, S. A., Tong, T., Fan, W., Zhao, H., Zhu, X., Mazzacurati, L., Li, X., Petrik, K. L., Fornace, A. J., Jr., Rajasekaran, B., and Zhan, Q. (2002) ATF3 induction following DNA damage is regulated by distinct signaling pathways and over-expression of ATF3 protein suppresses cells growth. *Oncogene* **21**, 7488-7496

Figure legends

Figure 1 Atf3 mRNA and protein is increased in cardiomyocytes exposed to ET-1 and suppressed by AS-Atf3

A - C, Cardiomyocytes were unstimulated (control) or exposed to 100 nM ET-1 for the times indicated (A) or were exposed for 0.5 h to 20 μ M cycloheximide (CHX), 10 μ M U0126, ET-1, or ET-1 in the presence of CHX or U0126 (B) or were exposed to ET-1 in the absence or presence of 2 μ M PD184352 (C). RNA was extracted and Atf3 mRNA expression measured by sqPCR (A and B) or qPCR (A and C). For A and B, representative sqPCR images are for Atf3 (upper image, 388 bp amplicon) and Gapdh (lower image, 412 bp amplicon). Positions of markers are shown on the left and controls with no reverse transcriptase (RT) were negative. Densitometric analysis for sqPCR of Atf3 is shown in the lower panels. In A, sqPCR and qPCR data are compared and results are a range from 0 (control values) to 1 (maximal expression at 0.5 h). All data were normalised to Gapdh and are means \pm SEM for 3 or 4 myocyte preparations. D, Cardiomyocytes were exposed to ET-1 for the times indicated and nuclear extracts (20 μ g protein) immunoblotted with antibodies to Atf3 using 12% polyacrylamide gels. Atf3 was detected as a band of \sim 21 kDa. A representative image

is shown (upper panel) with densitometric analysis (lower panel). Results are means \pm SEM for 3 myocyte preparations. E - G, Cardiomyocytes were infected with No-AS or AS-Atf3 AdVs at the indicated MOI and unstimulated (control) or stimulated with 0, 10 or 100 nM ET-1. Nuclear extracts were immunoblotted for Atf3 using 12% (E and F) or 10% (G) polyacrylamide gels. In G, the blots were divided into upper and lower sections and were probed with antibodies to Atf2 and Atf3, respectively. Atf2 was detected at \sim 70 kDa. @ $p < 0.05$ relative to ET-1, * $p < 0.001$ relative to control, ** $p < 0.01$ relative to control, # $p < 0.001$ relative to ET-1, (one way ANOVA with SNK post-test).

Figure 2 Infection with AdVs modulates expression of a subset of cardiomyocyte mRNAs

Cells (uninfected or infected with 150 MOI FLAG or AS-Atf3) were unstimulated or exposed to ET-1 for 90 min and RNA expression profiles determined using Affymetrix rat exon 1.0 ST arrays. A, Heatmaps show expression profiles for probesets that were significantly changed (>1.5 -fold, $FDR < 0.05$) by viral infection alone. Normalisation is to the gene median (range is -2.5 (cyan) through 0 (black) to +2.5 (red) on a log₂ scale). Results are means for 3 hybridisations each representing 3 independent myocyte preparations. Clustering on conditions and entities used a Euclidean distance matrix and centroid linkage ratio. B, Transcripts were classified according to function. Upregulated and downregulated transcripts are in red and blue, respectively. Transcripts regulated by interferons (Ifn) in other systems are in lighter colours.

Figure 3 Atf3 knockdown modulates the response of the cardiomyocyte transcriptome to ET-1

Cardiomyocytes were uninfected or infected with No-AS or AS-Atf3 AdVs (150 MOI), then were unstimulated (control) or exposed to ET-1 (100 nM, 90 min). RNA was extracted and analysed using Affymetrix rat exon 1.0 ST arrays. Analysis of transcripts that were upregulated (A) or downregulated (B) by ET-1 identified mRNAs that were significantly changed (>1.5 -fold; $FDR < 0.05$) by AS-Atf3 compared with No-AS or uninfected cells in the absence (clusters, A, B, C and F) or presence (clusters D, E and G) of a statistically significant baseline effect (>1.2 -fold) of viral infection as determined by GeneSpring analysis ($p < 0.05$). mRNAs were clustered as indicated. Heatmaps are shown for each cluster with normalisation uninfected controls (range: -2.5 (cyan) through 0 (black) to +2.5 (red) on a log₂ scale). Results are means for 3 hybridisations each representing 3 independent myocyte preparations. Clustering on entities used a Euclidean distance matrix and centroid linkage ratio. Histograms are means \pm SEM for the relative mRNA expression for each cluster. Each cluster was subjected to further statistical analysis independently of the global GeneSpring analysis. * $p < 0.001$ relative to No-AS ET-1, ** $p < 0.05$ relative to No-AS ET-1, # $p < 0.001$ relative to No-AS control, ## $p < 0.05$ relative to No-AS control, @ $p < 0.05$ relative to no virus control (one-way ANOVA with SNK post-test). (N.B. Although the No-AS effect in control cells is significant in the context of global statistical testing of microarray data, with the small numbers of genes in clusters D and E (with the variation in expression levels) this was not significant with secondary testing. Similarly, for cluster D, although the AS-Atf3 control data are significantly different from the no virus control, they are not statistically significantly different from the No-AS control).

Figure 4 qPCR validation of microarray data

Data were validated for Egr1 (A), Ptgs2 (B), Areg(C), Dusp5 (D), Dusp1 (E), Il1rl1 (F) and IL6 (G). Left panels, Cardiomyocytes were infected with No-AS (open circles, dashed line) or AS-Atf3 (closed circles, solid line) AdVs, then exposed to 100 nM ET-1 for the times indicated. RNA was extracted and expression of mRNAs analysed by qPCR. Results are means \pm SEM for 3 myocyte preparations. * $p < 0.05$ for AS-Atf3 relative to No-AS at the same time point (one-way ANOVA with SNK post-test). Right panels, Microarray data for each of the mRNAs studied are presented relative to uninfected (NV) controls. Results are shown for unstimulated cells (open bars) and cardiomyocytes exposed to ET-1 for 90 min (solid bars). Results are means for 3 independent myocyte preparations and hybridisations.

Figure 5 AS-Atf3 expression enhances expression of Egr1 protein in cardiomyocytes exposed to ET-1

Cardiomyocytes were uninfected or were infected with No-AS (open circles, dashed line) or AS-Atf3 (closed circles, solid line) AdVs, then exposed to 100 nM ET-1 for the times indicated. A, Nuclear extracts (20 μ g protein) were immunoblotted for Egr1 (upper images) or Atf3 (lower images). Representative blots of the same nuclear extracts are shown. B, Densitometric data for expression of Atf3 protein. C, Densitometric data for expression of Egr1 protein. Results were normalised to the no virus samples on each blot and are means \pm SEM for 3 myocyte preparations. *, $p < 0.05$ for AS-Atf3 relative to No-AS at the same time point (one-way ANOVA with SNK post-test).

Figure 6 Chromatin immunoprecipitation (ChIP) assays for binding of Atf3 to Egr1, Ptgs2 and IL6 promoters

Cardiomyocytes were unstimulated (control) or exposed to ET-1 (100 nM, 1 h). Promoter sequences with positions of PCR primers and potential Atf3 binding sites are provided in panels A (for Egr1), C (for Ptgs2) and E (for IL6) (coding sequence in bold text, underlined; 5' untranslated region in italics, underlined; positions of primers for PCR in bold, italics; potential ATF/CRE binding sites shaded and boxed). ChIP was performed using antibodies to Atf3 with sqPCR across Egr1 (B), Ptgs2 (D) and IL6 (F) promoters. Representative images for input DNA and ChIP DNA are provided (left panels) with densitometric analysis (right panels). Results are means \pm SEM for 3 myocyte preparations. * $p < 0.05$ relative to control (Student's *t* test). G, ChIP-PCR was performed for an unrelated sequence approximately 2000 bp downstream of the IL6 gene. The experiment was repeated with similar results.

Figure 7 Mathematical modelling of the Atf3-Egr1 feedback system in the cardiomyocyte response to ET-1

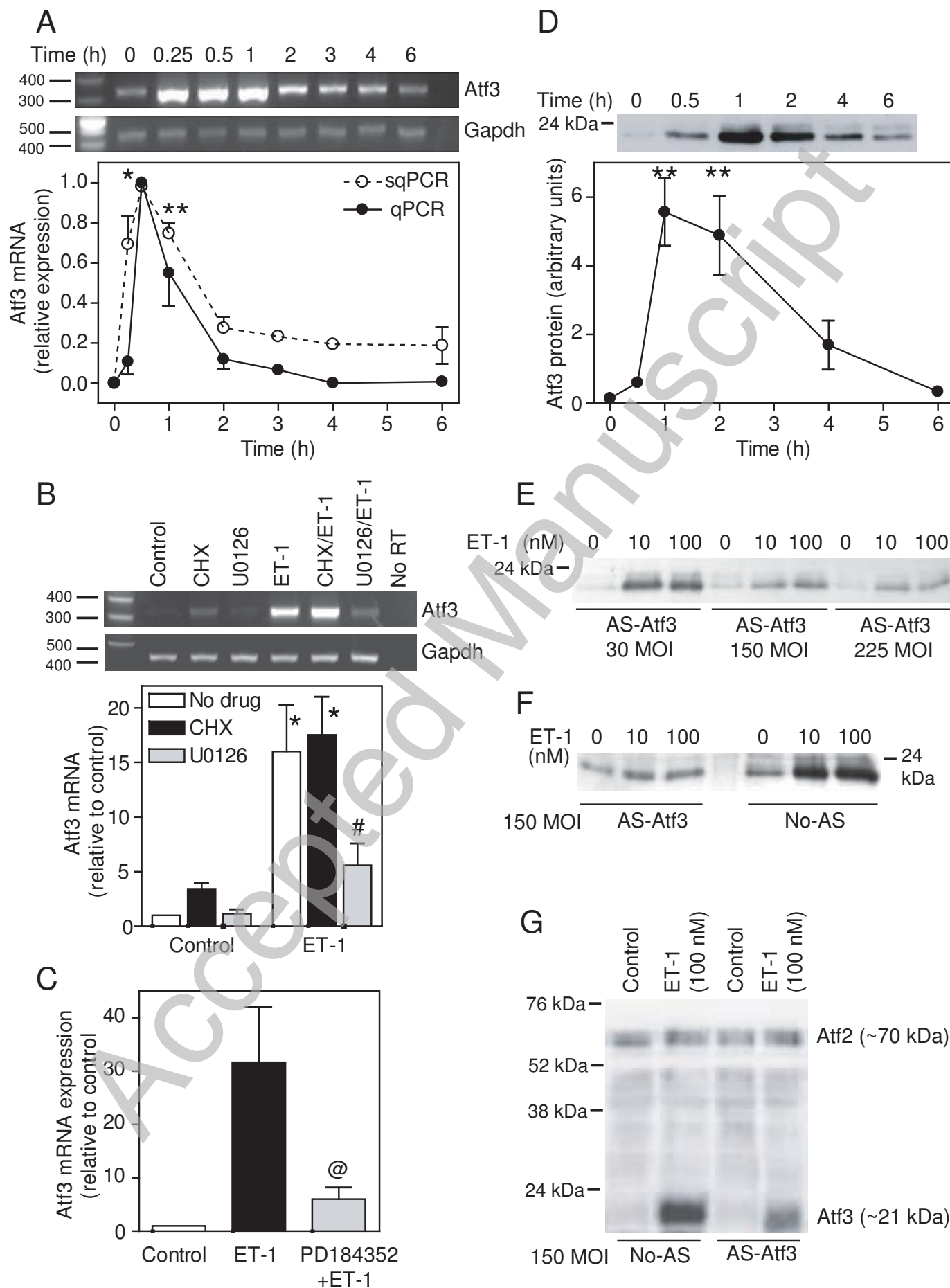
A, Schematic diagram of the system. ET-1 stimulates phosphorylation of MKK1/2 (MKK1/2-P) which phosphorylates and activates ERK1/2 (ERK \rightarrow ERK-P). ERK-P binds to transcription factors (not shown) on the promoters of Egr1 and Atf3 (Egr1 DNA, Atf3 DNA) to promote transcription and production of Egr1 mRNA and Atf3 mRNA. Atf3 mRNA is

translated into Atf3 protein that eliminates the positive signal from ERK-P on the Egr1 promoter. \emptyset denotes degradation. B, Results from the mathematical model derived for the schematic in A (see Supplemental Information, Mathematical modelling online) to show the rates of accumulation of MKK1/2-P (upper left panel), ERK-P (upper right panel), Egr1 mRNA (centre left panel), Atf3 mRNA (centre right panel), Atf3 protein (lower left panel) and the Atf3 protein/Egr1 DNA complex (lower right panel). The modelling was performed with (red, dashed line) or without (blue, solid line) feedback regulation of Atf3 on the Egr1 promoter. (N.B. No attempt was made to switch off either the initial signal from ERK1/2 or production of Atf3 mRNA).

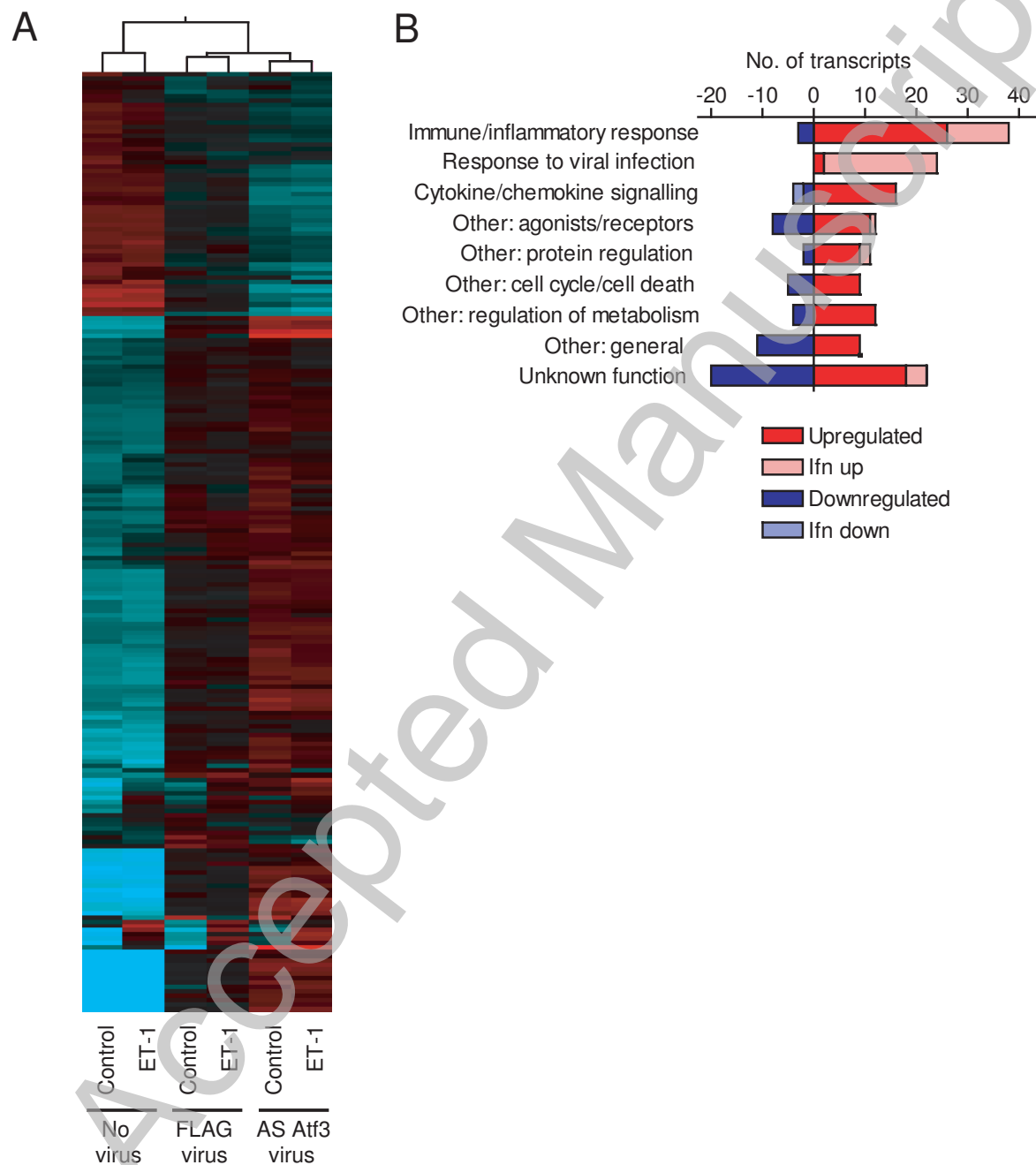
Figure 8 Atf3 is required for cardiomyocyte hypertrophy induced by ET-1

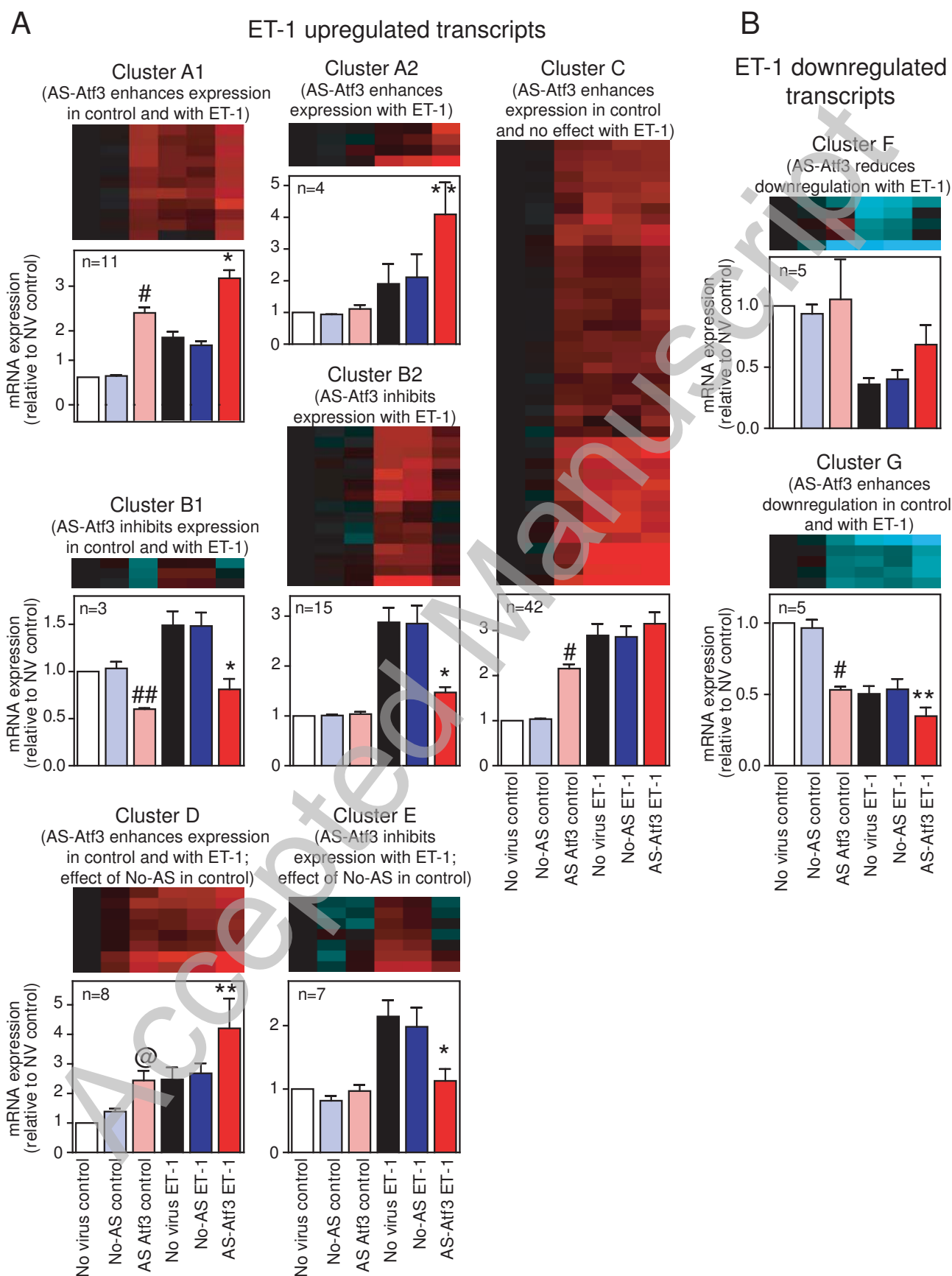
Cardiomyocytes were uninfected (A and B) or were infected with No-AS (C and D) or AS-Atf3 (E-H) AdVs, then unstimulated (Control; A, C, E and G) or exposed to 100 nM ET-1 for 24 h (B, D, F and H). Cells were immunostained with antibodies to troponin T. Results are representative of 3 independent experiments. Bar = 50 μ m.

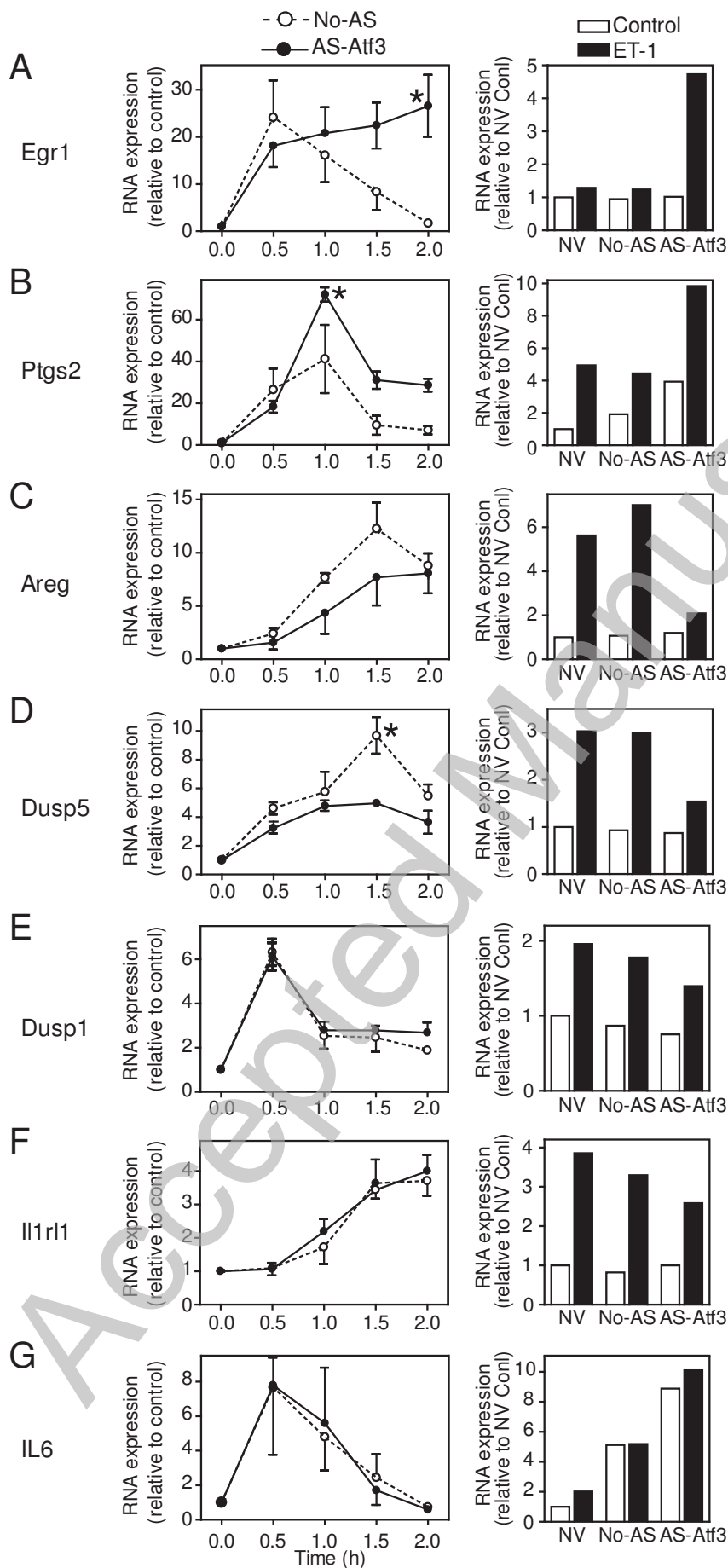
THIS IS NOT THE VERSION OF RECORD - see doi:10.1042/BJ20120125



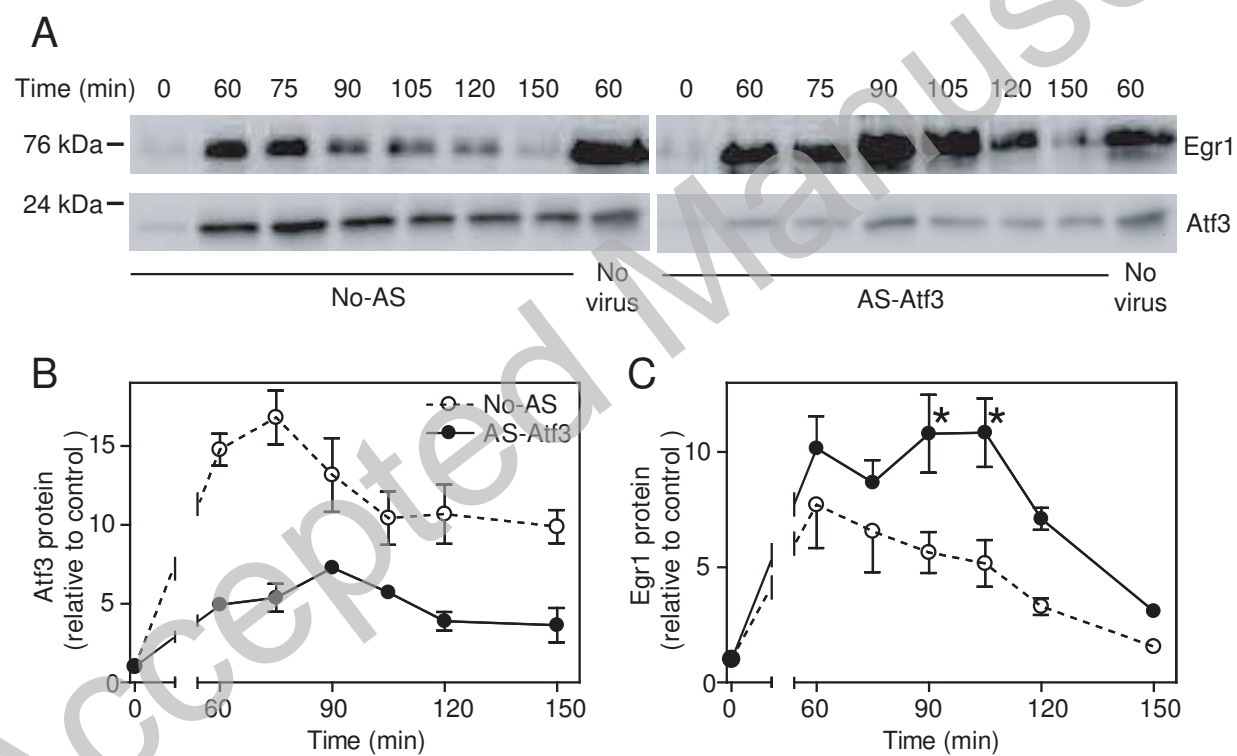
Giraldo et al Fig. 2.





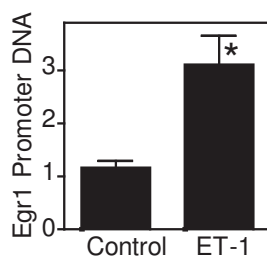
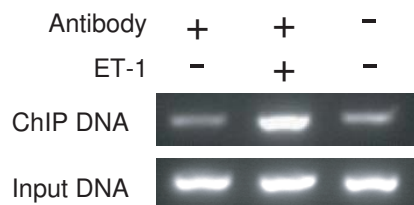


Giraldo et al. Fig. 5.

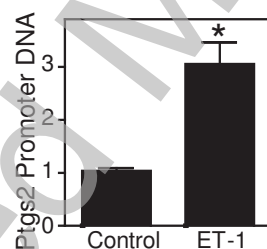
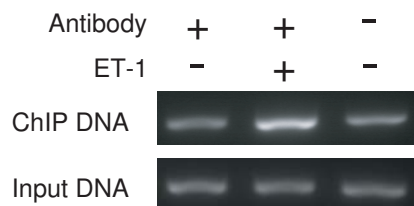


Giraldo et al. Fig. 6.

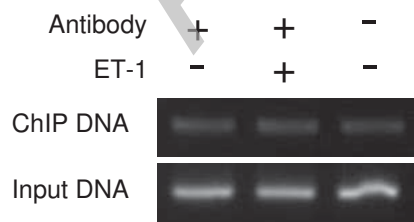
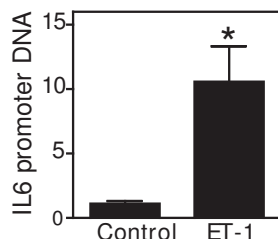
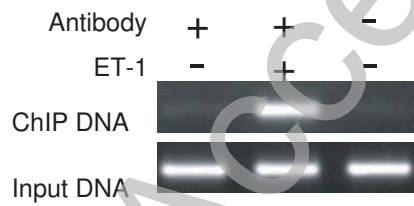
CACTGCCGCTGTTCCAATACTAGGCTTTCCAGGAGCCTGAGCGCTCAGGGTGCCGGAGCCGGTCGCAGGG
TGGAAAGCGCCACCGCTCTTGGATGGGAGGTC**TTCACGTCA**TCCGGGTCTCCCGGTCGGTCTTCCAT
ATTAGGGCTTCTGCTTCCCATATATGGCCAT**GTACGTCA**GGCGGAGCGGGGCCGTGCTGTTTCAGAC
CC**TGAAATAGAGGCCGATTTCG**GGGAGTCGC**GAGAGATCCAGCGCGCAGAACTTGGGGAGCCGCCCG**
CGATTGCGCGCGCGCCAGCTTCCGCCGCGCAAGATCGGCCCTGCCCGAGCCTCCGCGGCAGCCCTG
CGTCCACCACGGCGCGCGGCCACCGCCAGCCTGGGGGCCCACTACACTCCCGCAGTGTGCCCTGCAC
CCCCGATGTAAACCGGCCAACATCCGGCGAGTGTGCCCTCAGTAGCTTCGGCCCCGGGCTGCGCCACCA
CCCAACATCAGCTCTCCAGCTCGCACGTCCGGGATGGCAGCGGCCAAGGCCGAGATGCAATTGATGTCTC
CGTGCAGATCTCTGACCCGTTTCGGCTCTTTCTCTACTACCCACCATGGACA**ACTACCCCAACTGGA**



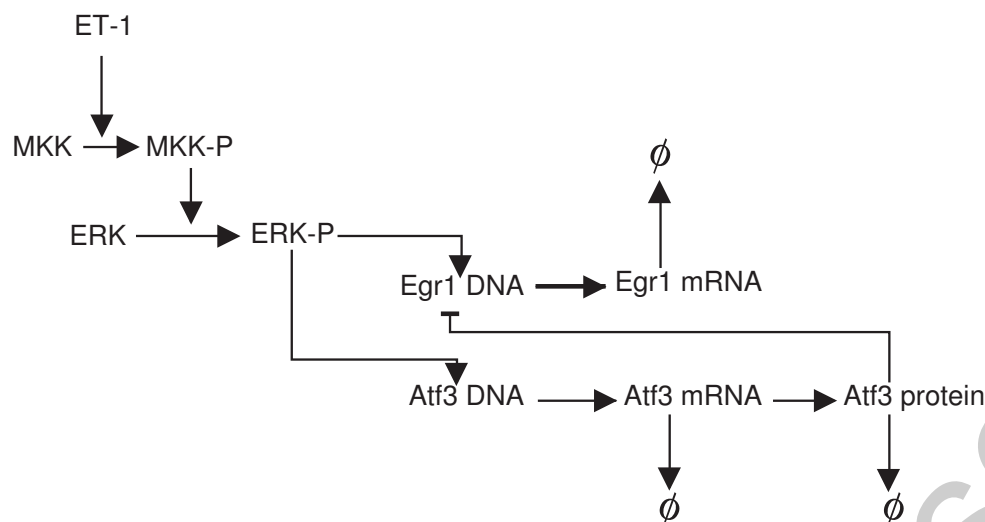
AGCAGCAAGCACGTCACTGCGCCCCAGTGGGGAGAGGCAAGGGGATTCCCTTAGTTAGGATCTGGAT
CCCGGGAGGGGAAGCTGTGACATTCTTGTCTCTCCGGCCCCCAGTGGATGCGGGACTGGGAGGAAAC
CCGA**GACCTCAAG**AGAGCCAGTCTTGGAGCAGGCACAGCGAACACAGGGCGCCTGGAAGGATGCAGAG
GGCGGTGCAGCTCTTGGCACCACTTGGGCAGCCGAGGGAAGCTTCTGGCTTCTTGGGCTCATTG
CG**TGAGTAAAG**CTGCCCTATGGGTATTATGCAATTGGAAGCGGAGATGGGGGAAAGCTGGGGGGGTGG
GGGGGTGGGGAAAGCCGAGGCGGAAAGACACAGTCA**GAAGTCACGT**GAGTCCACTTTACTAAGATTTA
AAAGCAAGGTTCTCCGGGTTAGCGGCCAGTTGTCAAAGTGAAGCGGAGAGCTTCAGGAGTACGAAGACCCCT
CCTACGAAGGAACTCAGCTCTGTGTCTGCCAGTCCCCCGCCAGCTTCACTGCCACCAACGCTGCCACA
ACTGTGCCACCACCGCTGCCACCTCTGCGATGCTCTTCCGAGCTGTGCTGCTCTGCCCTGCCCTGGCGC****



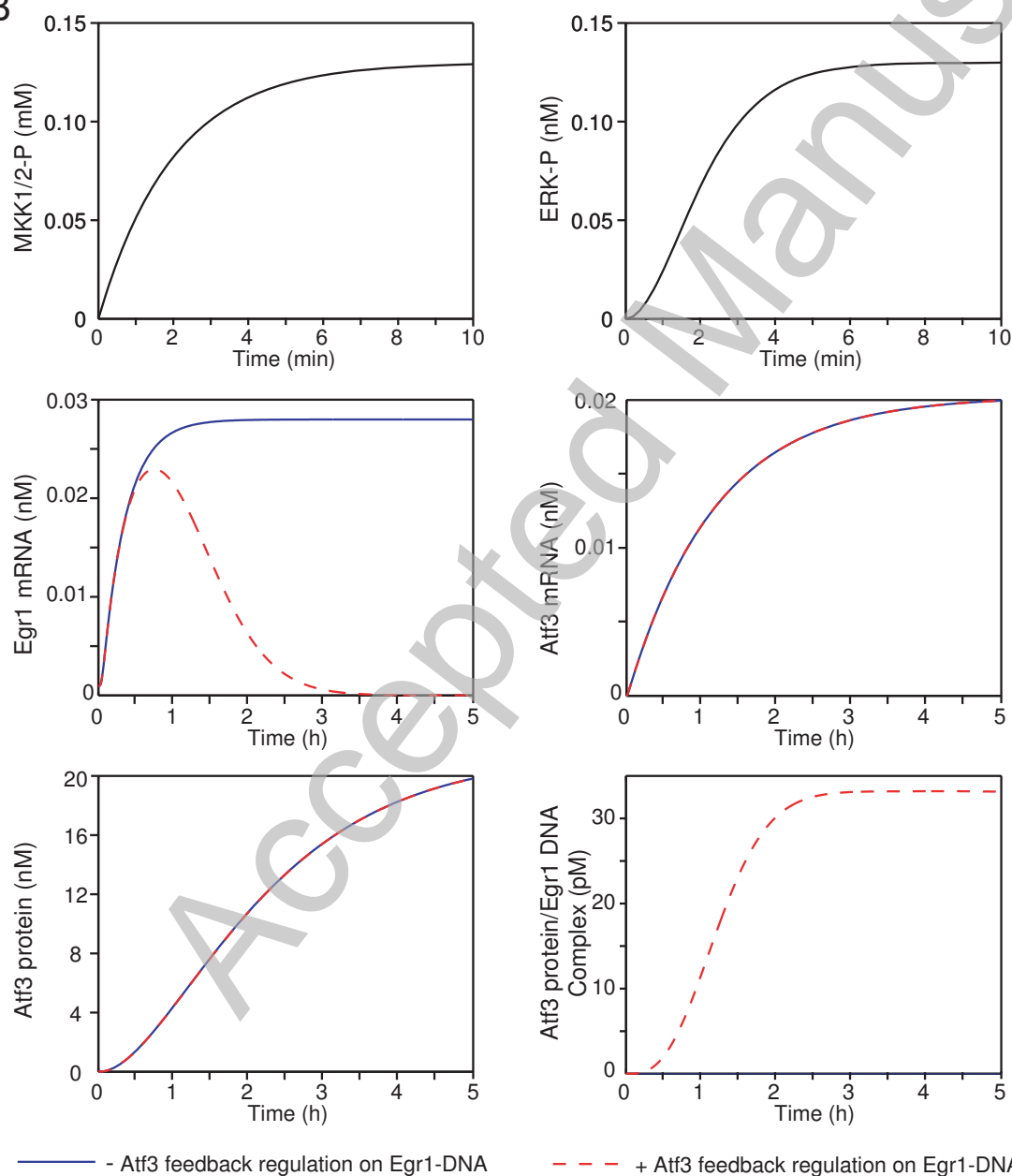
GTGCATTTTCAGTTTTTCCCCCTATCAAG**TGCTCAAGTGCTGAGTCACT**TTTAAAGAAAGAAAAAGAGTGA
TCAGGCTTCTTAAGGATAGCCTCAAGGATGACTTAAACACACTTTCCCCCTCCTAGCTGTGATTCTTTGG
ATGCTA**AATGACGTCA**CATTGTGCAATCTTAATAAGGTTTCCAATCAGCCCCACCCACTCTGGCCCCACC
CCCCACCTCCAACAAAGATTTTTATCAAATGTGGGATTT**CCCATGAGTCT**CAAAAGTAGAGAGTCGACT
CCCAATAAATATGAGACTGGGGATGCTGTG**AGCTCA**TTCTGTCTCGAGCCCACCAGGAACGAAAGTCAAC
TCCATCTGCCCTTCAGGAACAGCTATGAAGTTTCTCTCCGCAA****



A



B



Giraldo et al. Fig. 8.

